ORIGINAL CONTRIBUTION

Investigating Joint-Free Mechanical Systems with PLA and ABS Materials Using the Fuse Deposition Modelling Method

R. N. Chikkangoudar[1] · Chetan Patil[2] · R. N. Panchal[3] · Sonal Shamkuwar[4] · Mahesh M. Kawade[5] · Shrishail B. Sollapur[6] · G. Veeresha[7] · Prakash Kumar[8]

Abstract In recent times, the growing popularity of joint-free mechanical systems and structures is attributed to advancements in 3D printing technology. Unlike traditional mechanically joined systems, 3D-printed products require fewer fasteners. However, the widespread adoption of additive manufacturing in the mechanical industries is hindered by limitations in handling various engineering materials. Currently, only a restricted range of ductile and plastic materials is utilized in additive manufacturing processes. This study aims to replace adhesive bonding and bolt joints with an innovative approach involving equivalent geometrical layers. The strength of these joints is intended to be achieved through careful consideration of layer thickness and geometry. The research investigates the strength of conventional lap joints, such as adhesive-bonded or bolted joints, across different materials. Finite element models of these ASTM specimens will be developed in ANSYS for static analysis and comparison. The ultimate goal is to establish an equivalent design procedure that replaces traditional joints with layers of materials through the additive manufacturing process. To validate this approach, a quadcopter structure was designed using 3D printing technology, fabricated with ABS and PLA materials, assembled, and flight-tested to achieve a thrust-to-weight ratio of nearly two. The successful validation of the design demonstrates that 3D-printed additive manufacturing is a valuable technology for constructing lightweight and high-performance UAV structures. Notably, the quadcopter frame was produced as a single component, streamlining the assembly process compared to traditional assemblies consisting of eight to ten parts.

✉ Shrishail B. Sollapur
  shrishail.sollapur@gmail.com

  R. N. Chikkangoudar
  chikkangoudar@gmail.com

  Chetan Patil
  chetan.patil@mitwpu.edu.in

  R. N. Panchal
  rnpanchal0@gmail.com

  Sonal Shamkuwar
  sonal.shamkuwar@viit.ac.in

  Mahesh M. Kawade
  mahesh.kawade@moderncoe.edu.in

[1] Department of Mechanical Engineering, KLE Technological University. Dr. M S Sheshgiri Campus, Belagavi, Karnataka 590008, India

[2] Department of Mechanical Engineering, Dr. Vishwanath Karad MIT WPU, Pune, Maharashtra 411038, India

[3] Department of Mechanical Engineering, JSPM's Rajarshi Shahu College of Engineering Tathawade, Pune, Maharashtra, India

[4] Department of Mechanical Engineering, Vishwakarma Institute of Information Technology, Pune, Maharashtra 411046, India

[5] Department of Mechanical Engineering, PES's Modern College of Engineering, Savitribai Phule Pune University, Pune, Maharashtra 411005, India

[6] Department of IIAEM and ME, Faculty of Engineering and Technology, JAIN (Deemed -to- be University), Bengaluru, Karnataka 560069, India

[7] Department of Mechanical Engineering, New Horizon College of Engineering, Bengaluru, Karnataka, India

[8] Department of Metallurgical and Materials Engineering, National Institute of Technology, Jamshedpur, Jamshedpur, India

Introduction

Mechanical system and components are manufactured using elastic materials (ductile) through conventional machining operations such as lathe, drilling, boring, countersinking, etc., where the tolerance level approximately achieved is 100 microns [1–3]. Mechanical components (for example, bar, beam, and plate) are joined by mechanical joints like rivets, bolts, welding and adhesives. Stainless steel, mirage steel, aluminium, titanium, cast iron are some of the metallic materials most commonly used in making mechanical systems [4–6].

The advancement in computing technology has changed the manufacturing process by introducing computer sided manufacturing (CAM), namely CNC machining (Computer Numerical Control), which has improved the performance of the machining ability of obtaining complicated shape with high degree of accuracy and tolerance level of 5–10 microns [7–10]. In conventional machining, the workmanship of a technician plays a major role in order to machine the components with high degree of accuracy. In this process, a 2-D drawing is usually employed, while machining the component to obtain specified dimensions [11–13], whereas the CNC machine reads the CAD model of the component, including the required dimensions and tolerances directly into the computer [14–17]. The components made either by conventional or CAM have to be joined in order to fabricate any real-time mechanical system, for example, aircraft wing structure with engine, unmanned air vehicles (Quad copter, fixed wing UAV) and chassis of automotive, etc. The mechanical joints play a vital role for machining the integrity of all the subsystems, besides resisting the applied loads. Designing of suitable mechanical joints is a major challenge as it involves knowledge from the subjects of mechanics of materials, design of machine elements, manufacturing process and behaviour of mechanical system under static and dynamic loadings [17–24].

When the joints approach failure, the complete mechanical system will collapse. Therefore, proper precaution and sufficient care must be taken, while designing the joints to transfer the loads appropriately [25–29]. In recent times, a new manufacturing process called additive manufacturing has emerged. It is also known as 3D printing technology, in which the materials are joined or solidified to create a 3D object through computer-controlled data flow. Here, the material is being added together by layer by layer, which is why the name additive manufacturing has come [30–34]. Objects of different shape and geometry can be achieved and produced by CAD model drafting. Unlike material removal in conventional machining process, additive manufacturing builds a dimensional object by successfully adding by layer-wise procedure. There are various advantages expected in the additive manufacturing; however, research works are being pursued to improve additive manufacturing so that the majority engineering materials can be used in the manufacturing process [28–30].

Methodology

A systematic methodology is followed to build and test the joint-free 3D-printed quadcopter. Figure 1 illustrates the stepwise building process of joint-free 3D-printed quadcopter.

Specimen Testing

The quadcopter, unlike a standard helicopter, lacks a tail rotor for yaw motion control. It has four motors, two of which rotate clockwise and two of which rotate anticlockwise. When the clockwise motors spin faster than the anticlockwise ones, a moment is generated around the yaw axis.

BLDC Motors

Brushless direct current (BLDC) motors communicate without the need of brushes, instead depending on electronic commutation. These motors have important benefits, such as excellent speed-to-torque characteristics, high efficiency, noiseless operation, and a wide speed range, all of which contribute to a longer lifespan. An electronic speed controller is required to regulate the motor. The lack
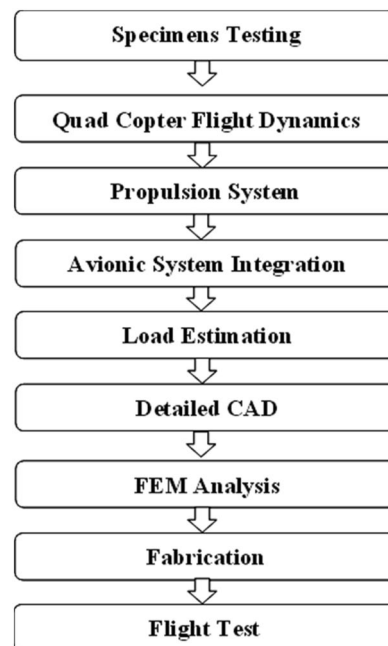

Fig. 1 Building process of joint-free 3D-printed quadcopter

of brushes leads in a longer motor life, avoiding sparking and decreasing electrical noise. Four BLDC motors are often used in quadcopters. BLDC motors are commonly designated in KV, for example, 850kV, 1400kV, and 1800kV. The KV rating of a motor specifies its revolutions per minute (RPM) per volt applied—for example, a 1000kV BLDC motor would revolve at 1000 RPM with 1 V and 12,000 RPM with 12 V supplied.

Propellers

Each brushless motor on the quadcopter is equipped with a propeller, although the four propellers differ. The front and rear propellers of a quadcopter are inclined to the right, while the left and right propellers are tilted to the left. This configuration, which involves propeller pairs with opposing tilts in each direction, guarantees that all propellers create lifting power while not rotating in the same direction. This design makes it easier to stabilize yaw rotation, or rotation around the quadcopter's vertical axis.

Flight Mechanism

A quadcopter is a small vehicle with four propellers positioned on a rotor in the centre of a cross frame. The vehicle's motion is controlled by fixed-pitch rotors in this system. The essential characteristic is the independence of

Fig. 2 Euler axis reference frame of quadrotor

the four rotor speeds. This independence allows for simple management of the vehicle's pitch, roll, and yaw attitudes, as shown in Fig. 2.

Quadcopter Hovering

When the upward lift equals the downward pull of gravity, hovering occurs. To climb, the drone (quadcopter) requires a lift force larger than gravity, which is done by raising the RPM (speed) of all four propellers at the same time, creating additional lift. To descend, RPM is reduced on all four propellers at the same time. The controller, which is controlled by the left stick, regulates the rotor RPM to raise or descend the quadcopter.

Changing the angle of the lifting force introduces both vertical and horizontal components for lateral and forward/backward motions. The vertical component keeps the quadcopter aloft, while the horizontal component gives the drone control thrust, allowing it to move left, right, forward, or backward.

Quadcopter Motion

The pitch of the quadcopter is controlled using the right stick on the controller to create forward or backward motion (as shown in Fig. 3). This modification involves lowering the RPMs of the front propellers while raising the RPMs of the back propellers. As a result, the lift force gets a horizontal component, propelling the quadcopter forward. To make the quadcopter travel backward, raise the RPM of the front propellers while decreasing the RPM of the back rotors. A similar change in RPM happens to manoeuvre the quadcopter sideways; however, this time it includes the left and right propellers (as shown in Fig. 3). To move the drone to the left, reduce the RPM on the left rotors while raising the RPM on the right. To shift the quadcopter to the right, a comparable change in rotor RPMs is made.

Flight Control System

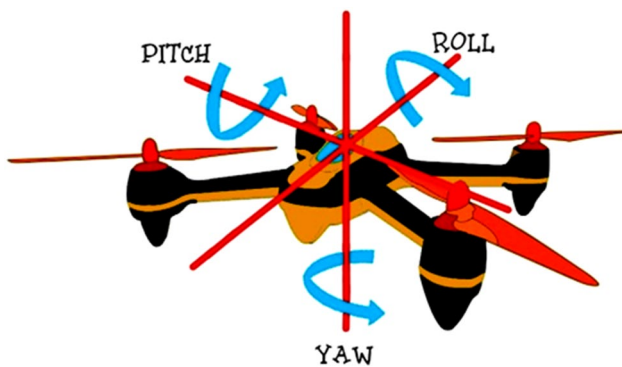The quadcopter flies and moves by varying the RPMs of each propeller. When you move a stick on your controller,
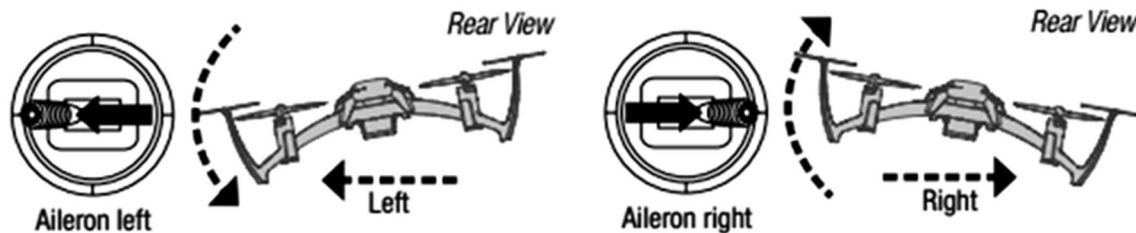

Fig. 3 Stick inputs versus vehicle

the input must be converted into orders for each of your quadcopter's four motors. The flight control system does this translation. The flight control computer is critical in simplifying the control of all four propellers necessary to enable your drone to fly. Furthermore, the flight control computer may communicate with a variety of different equipment and sensors. Its principal link is with the remote-control receiver, which is connected to your remote transmitter. The flight controller in sophisticated quadcopters is integrated with a transmitter, allowing two-way communication with your controller. This feature improves communication between the drone and its remote controller. Furthermore, modern quadcopters frequently include a variety of sensors to improve their functioning. GPS for accurate locating, a gyrocompass for orientation and stability, and a barometer for altitude measurement are examples of these sensors. These powerful sensors help the quadcopter's navigation, stability, and overall performance.

Quadrotor Frame

There are several commercial quadrotor frame variants, including H, X, and Hybrid-X. The frame size is determined by the total weight, with an increase in frame weight equating to an increase in material utilization. The majority of the components required for the build are dictated by the frame size. Furthermore, the maximum propeller size that a tiny quadcopter frame can allow may be used to determine its size. A "210 frame" or a "5-inch frame", for example, indicates compatibility with 5-inch propellers, as those are the largest props it can efficiently turn. A 180-class frame with a propeller diameter of 4 inches and a frame size ranging from 150 to 200 mm has been chosen for the construction of a 3D-printed quadcopter.

Propulsion System

The below diagram (Fig. 4) shows the flow of commands from the flight control board to the propulsion system. The propulsion system is the driving force for the quadrotor. The motors used are brushless DC motors.

Brushless direct current (BLDC) motors communicate without the need of brushes, instead relying on electronic commutation. Their key benefits are excellent speed versus torque characteristics, great efficiency with noiseless operation, and a broad speed range that contributes to a longer lifespan. These motors require electronic speed controllers (ESCs) to be controlled. BLDC motors have a substantially longer life due to the lack of brushes, with no sparking and minimum electrical noise. Four BLDC motors are often used in quadcopters. BLDC motors are commonly rated in KV increments of 850, 1100, 1400, and 1800. The revolutions per minute (RPM) per volt applied to the motor are indicated by the KV rating. A BLDC motor with a KV rating of 1000, for example, will revolve at 1000 RPM when 1 V is provided and at 12,000 RPM when 12 V is applied. Pulse width modulation (PWM) signals, which are square digital signals, are often used to operate BLDC motors because they produce an analogue-like signal using digital methods. PWM signals are interpreted by speed controllers and converted into three-phase signals that are supplied to BLDC motors. This three-phase signal corresponds to an angular velocity (w) order. The motor's behaviour is governed by both electric and mechanical dynamics, as shown in Fig. 5 and Table 1.

Propellers

A propeller is installed on each of the brushless motors. The front and rear propellers of a quadcopter are inclined to the right, while the left and right propellers are tilted to the left. By designing the propeller pairs with opposite tilting in each direction, they provide lifting thrust without rotating in the same direction. This design enables the quadcopter to efficiently stabilize yaw motion (rotation around its vertical axis). The employment of four 4045 tri-blade propellers is also noteworthy in the context of the propulsion system. The unique design and specifications of these propellers (40 mm diameter, 4.5-inch pitch, and three blades) contribute to the overall performance and efficiency of the quadcopter's propulsion system.

Electronic Speed Controller

The speed controller takes input from the flight control board and converts the signal into the current required by
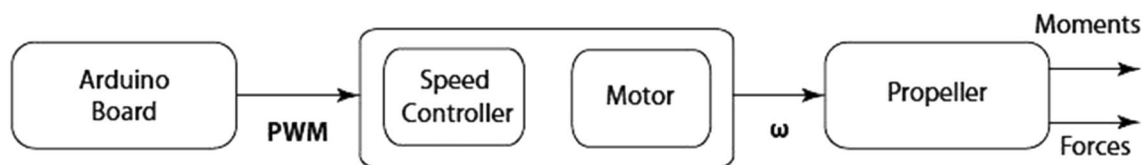

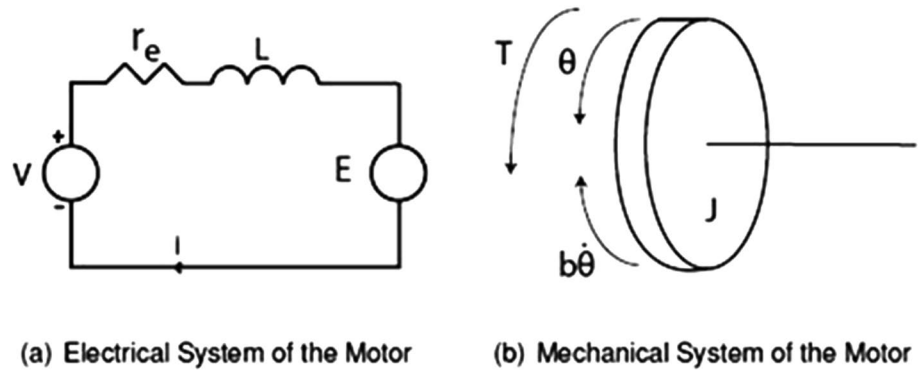**Fig. 4** Propulsion system

Fig. 5 Principle of motor

(a) Electrical System of the Motor   (b) Mechanical System of the Motor

Table 1 Selected propulsion system for 3D-printed quadcopter

Model	Figure	Quantity	Weight in grams
Avionic M2024 KV2400 MICRO brushless motors		4	14

the brushless motors. A 20 amp 2-4S lipo ESC is selected for quad.

Avionics System Integration

Flight Controller

The flight controller is the brain of the quadrotor which houses an inertial measurement unit and a controller. The pilot input signals are processed on board, and the corresponding PWM signals are sent to the motor via the electronic speed controller. With a 32bit ST microprocessor and a host of equally impressive sensors, this Rev6 Arco version comes with 16mbit memory and the BMP280 barometer.

Power System

LiPo batteries are dependable on what motors running. For 1306 3100 kV motors 2S and 3S are the most common. It is possible to run 4S on it, but it is a bit unstable due to the stress, and motors might not last long. Any larger motors such as 1806/2204 2300 kV motors is suitable. Capacity wise, 1000–1500 mAh are good range for 180 size mini-quad.

Considering the all the subsystems of quadcopter and materials used for subsystem total weight is estimated

Table 2 Subsystem weights

Subsystem	Details	Weight(gms)
Structure	PLA	85
	ABS	101
Battery	LiPo cell 1500 mAh	115
Avionics	ESC(40) + control board(20) + power distribution Board(8)	68
Propulsion	Brushless motor + prop + adapter	48–110
Payload		50
Total weight		382–444

as shown in Table 2. The weight breakdown of entire quadcopter is shown in Fig. 6.

Load Estimation

- **Propulsive Forces:** These forces are generated by the thrust produced by the four motors.
- **Gravitational Forces:** This force is the downward weight of the vehicle.

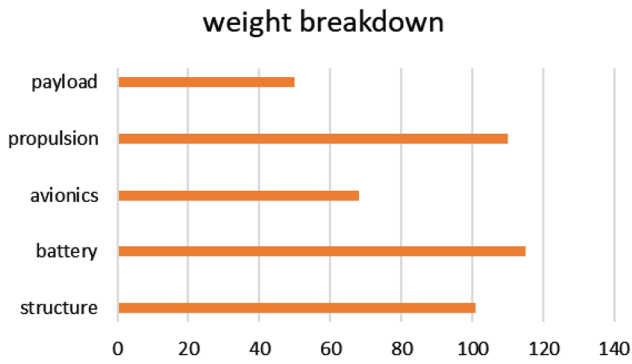Total force and moments acting on the vehicle are shown in Fig. 7.

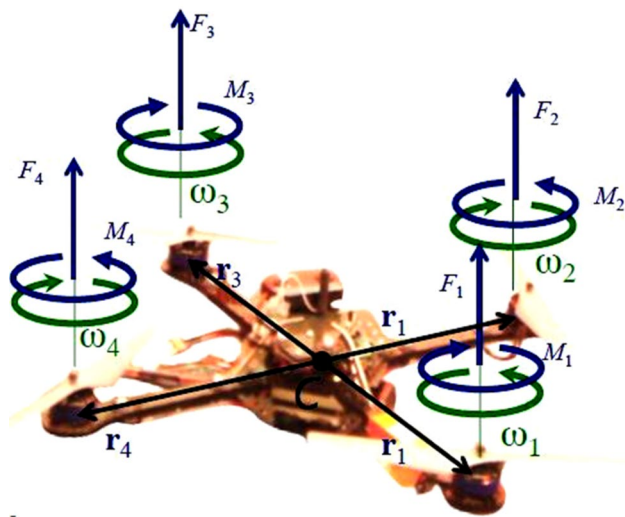**Fig. 6** Total weights breakdown chart

Fig. 7 Total force and moments acting on the vehicle

Propulsion System

Ideal thrust-to-weight ratio for quadcopter is considered to be 2–2.5. If the all-up weight of the vehicle is estimated to be 1 kg, the propulsion system must be able to generate thrust greater than the all-up weight to lift off the ground and hover at a particular altitude. Considering T/W ratio as 2, the overall thrust produced by the system should be 2 kgs which corresponds to around 500 g thrust at 50% throttle per motor as shown in Fig. 8. In present study, the selected propeller was tested with its motor system and found that each one would develop around 190 gms thrust. Therefore, all the four motors could generate 760 gms of total thrust and thus T/W of 2.05 is achieved.

Selection of Components

A quadcopter is a tiny vehicle with four propellers connected to a rotor placed at the cross frame. The vehicle's motion is controlled by fixed-pitch rotors, with the speeds of these four rotors being independent. The overall weight of the quadcopter is computed and reported in Table 3 after taking into account all of the subsystems and the materials utilized for each subsystem.

Development of CAD Model

Considering the all-subsystem 3D model is generated using the CATIA V5. Figure 9 shows the isometric view of bare quadcopter (without any electronic and electrical components). Assembled isometric view of quadcopter is shown in Fig. 9. The mechanical and physical property for
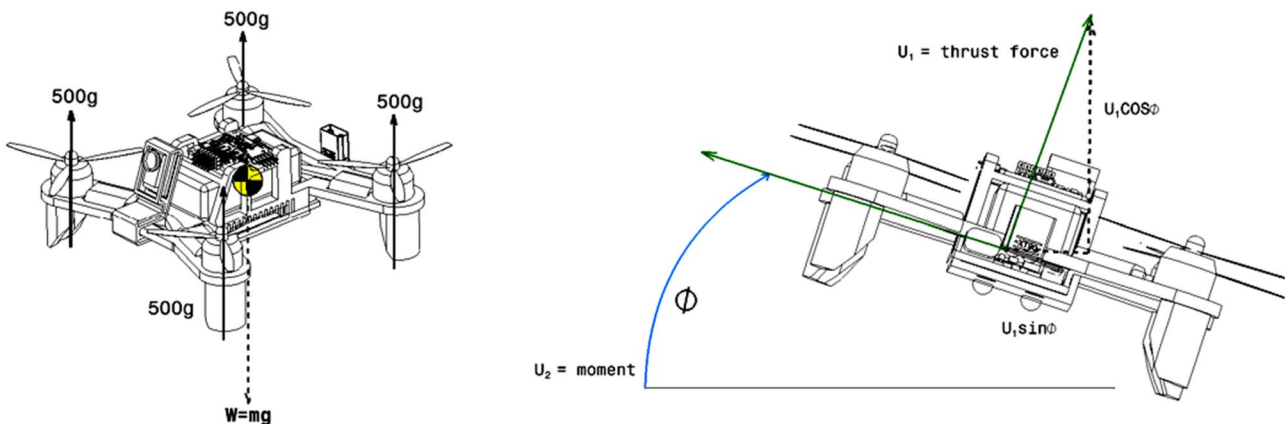

Fig. 8 Maximum thrust hover and rolling/pitching manoeuvre conditions

Table 3 Selected propulsion system for 3D-printed quadcopter

Model	Quantity	Weight in grams
Avionic M2024 KV2400 MICRO brushless motors	4	14
Propeller	4	110
Flight controller	1	11
Electronic speed controller	1	23
Power system	1	18

Table 4 Properties of ABS material

Property	ABS
Young's modulus (GPa)	2.6
Tensile strength (MPa)	45
Density (g/cc)	1.16
Flexural strength (MPa)	81
Poisson's ratio	0.35
Ultimate strength (MPa)	40

Table 5 Frequency chart

Mode no	Frequency (Hz)
1	Rigid body mode
2	Rigid body mode
3	Rigid body mode
4	Rigid body mode
5	Rigid body mode
6	Rigid body mode
7	144.9
8	202.7
9	259.4
10	366.9

ABS (Acrylonitrile Butadiene Styrene) is given in Table 4. The finite element model of the 3D-printed quadcopter is made using tetra mesh in HYPER mesh software.

Fig. 10 CAD model of quadcopter

Simulation and Analysis

Ideal thrust-to-weight ratio for quadcopter is considered to be 2–2.5. In present study, the selected propeller was tested with its motor system and found that each one would develop around 190 gms thrust. Therefore, all the four motors could generate 760 gms of total thrust and thus T/W of 2.05 is achieved. Figure 10 shows a CAD model of the designed quadcopter.

Free vibration analysis is carried out without constraint. There are 6 rigid body modes which are appeared because of free–free conditions. In that, there are three translations and three rotations about x-, y-, z-axes, respectively, as shown in Table 5.

The elastic mode shapes, i.e. the dynamic deflected shape in different frequencies, are shown in Fig. 11. Two boundary conditions are considered (Fig. 12). The first one is as though the quadcopter is simply supported on the ground and other is held at the C.G. The results are presented in this section (Figs. 13 and 14). The static analysis results show that the margin of safety is more than 10, considering the ultimate strength. Therefore, the deigned quadcopter is safe against the propeller loading, i.e. 800 gms. Also, it can carry the pay loads safely [35–40]. The joint-free structure is safely carrying the loads and deforms elastically. Thus, this design is recommended for 3D printing with ABS material. However, if PLA material is used, then there is further scope for weight reduction, as its Young's modulus is higher than ABS [41–47].

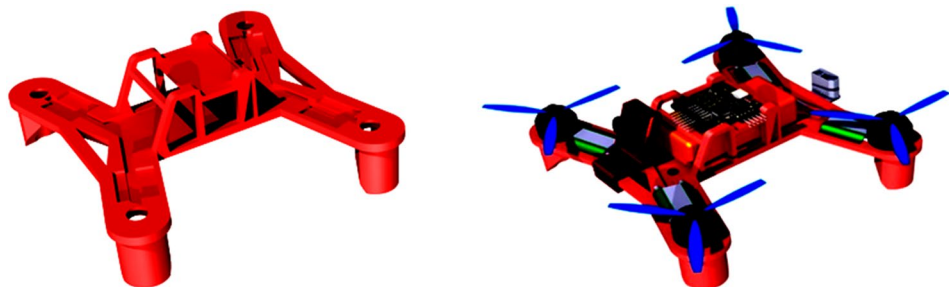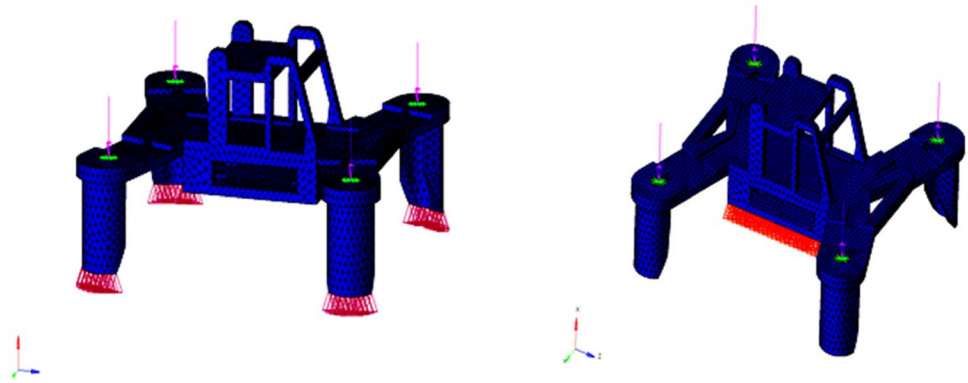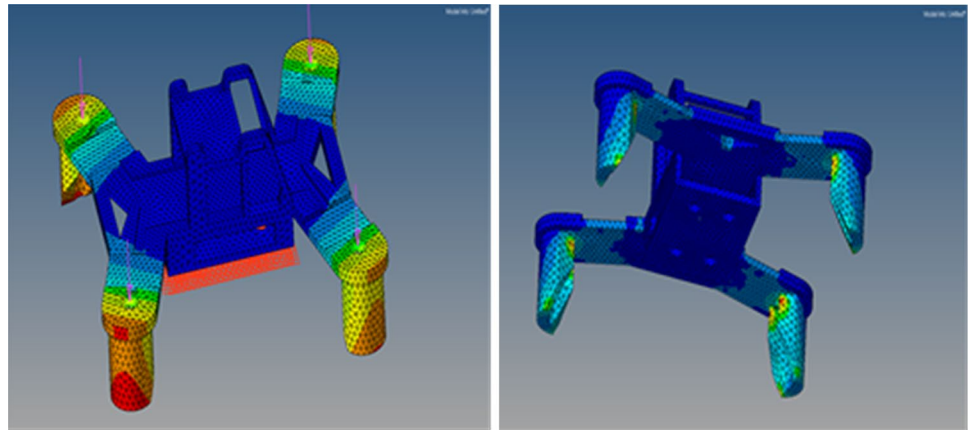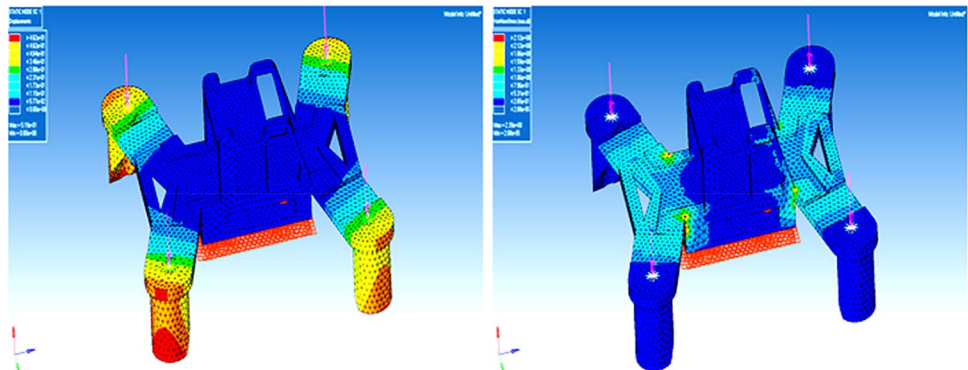**Fig. 9** Isometric view of quadcopter without electronic components and isometric design for assembly

Fig. 11 Static analysis

Fig. 12 Boundary conditions; simply supported and at CG

Fig. 13 At CG: FE simulations of displacement and stress

## Fabrication Through Additive Manufacturing

Figure 15 shows the fabricated model of the quadcopter using Plasto 600 3D printer. It is to be noted that it is manufactured as a single component using ABS material, in which lap and bolted joints are avoided. ABS is common thermoplastic polymer. Also, the weight of the copter frame is around 75 gms, which is less than 10% of the total thrust of the copter (800 gms) with 100% throttle [48–53]. It is worth noticing that the conventional manufacturing methods would normally provide quadcopter around 30% of all-up weight. Therefore, one can understand the advantages of reducing the structural weight of the copter. The present design has a very high factor of safety that is 10. However, for flying structure, normally 1.5 is sufficient. Therefore, there is scope to improve the T/W ratio by optimizing the quadcopter frame [54–60].
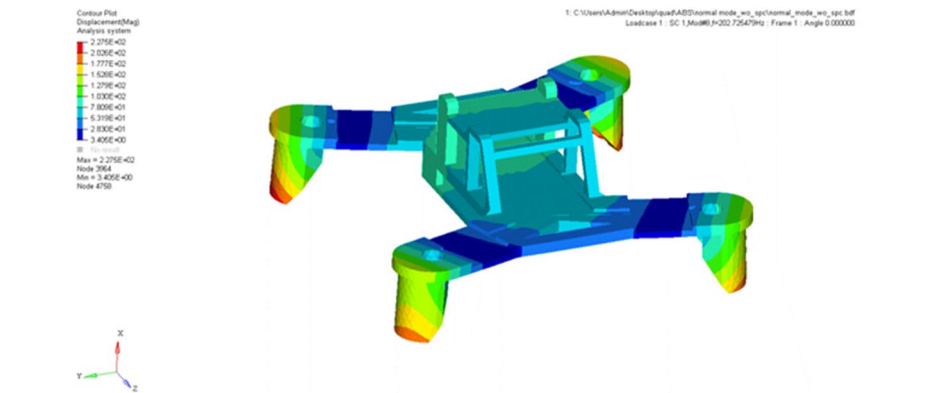
Testing

The developed quadcopter was flight-tested, after integrating all the subsystem in indoor. Figure 16 shows one of the initial flight trails.
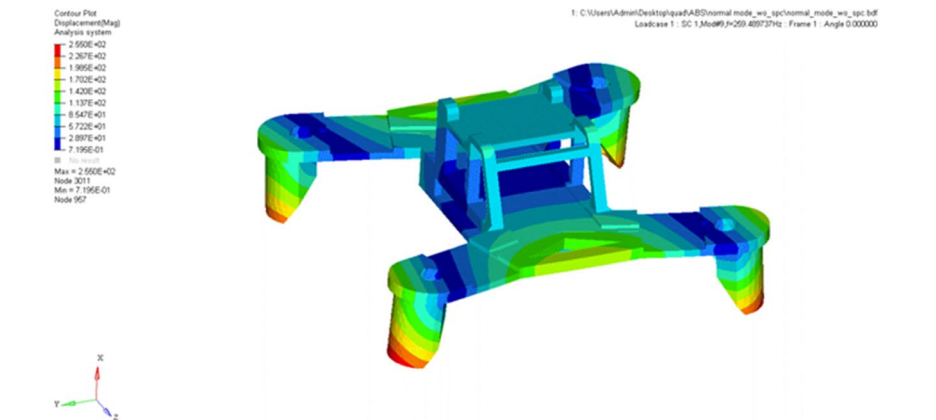
Fig. 14 Modal analysis
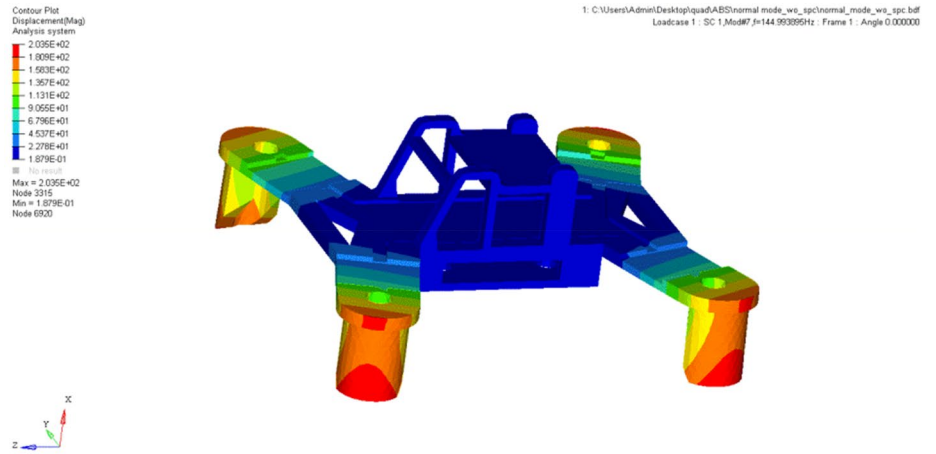
Mode 7

Mode 8

Mode 9

Fig. 15 3D-printed quadcopter

Fig. 16 Indoor flight testing

The successful flight of the quadcopter has demonstrated the quality of the design, 3D-printed frame structure to carry the loads, and a stable flight on hovering mode. This kind of vehicle can monitor, taking images very closely the operations of the machines in hop floor and measure the noises [61–67].

Conclusions

In this work, the 3D printing technology is used to achieve a thrust-to-weight ratio of 2.0 in a quadcopter design. As a first step, a typical 3D printing material, namely ABS, has been chosen and its material property is obtained through tensile testing machine in UTM. Subsequently, a conventional adhesively bonded lap joint specimen and a completely 3D-printed joint-free specimen are tested to evaluate the shear strength of the bonding region. 3D-printed joint-free test has shown encouraging result because it does not have any bonding material. Also, this specimen is made only 50% infill. So, there is a scope to improve the shear strength of 3D-printed structure by fine tuning the infill content and optimizing the thickness. Further, using the knowledge generated, a 3D quadcopter frame is designed as a single component, unlike conventional manufacturing which may involve 8–10 components. CATIA V5 software is used for this purpose. Finite element analysis is carried out to validate the design, and the same is 3D printed as frame using ABS material. It took 36 h of printing the complex geometry.

Declarations

Conflict of interest   The writers claim that there are not any conflicts of interest.

References

1. J.E. Shigley, C.R. Mischke, T.H. Brown Jr., *Standard Handbook of Machine Design* (McGraw-Hill Education, 2004)
2. B. Gireesh, B. Sollapur Shrishail, V.N. Satwik, Finite element & experimental investigation of composite torsion shaft. Int. J. Eng. Res. Appl. **3**(2), 1510–1517 (2013)
3. Best Quadcopter Reviews— Drones and Multirotors—Drone Omega.com. Accessed 11 February 2023, 9.30 am
4. O.B. Deore, Design and analysis of complaint mechanism using FEA. Development 7(10):1–4 (2020).
5. M. Groover, E.W.J.R. Zimmers, *CAD/CAM: Computer-Aided Design and Manufacturing* (Pearson Education, 1983)
6. D.D. Baviskar, A.S. Rao, S. Sollapur et al., Development and testing of XY stage compliant mechanism. Int. J. Interact. Des. Manuf. (2023). https://doi.org/10.1007/s12008-023-01612-1
7. B. Bhattacharyya, B. Doloi, *Modern Machining Technology: Advanced, Hybrid, Micro Machining and Super Finishing Technology* (Academic Press, 2019)
8. S. Gunjawate, Structural analysis and topology optimization of leaf spring bracket. Int. J. Eng. Res. Technol. (IJERT) **9**(7), 1448–1494 (2020)

9. M.S. Patil, S.P. Deshmukh, Position estimator algorithm implementation on precision applications. Mater. Today Proc. **24**, 333–342 (2020)

10. S.B. Sollapur et al., Experimental investigation of high precision XY mechanism. Int. J. Mech. Eng. Technol. **9**(5), 43–50 (2018)

11. M.S. Patil, S.P. Deshmukh, Design and development aspects of flexure mechanism for high precision application. In AIP Conference Proceedings, vol 1943. no. 1, (AIP Publishing, 2018)

12. I. Zeid, *CAD/CAM Theory and Practice* (McGraw-Hill Higher Education, 1991)

13. U.A. Khilare, S.B. Sollapur, Investigation of residual stresses and its effect on mechanical behaviour of AISI310.

14. T. Shinde et al., Fatigue analysis of alloy wheel using cornering fatigue test and its weight optimization. Mater. Today Proc. **62**, 1470–1474 (2022)

15. D. Saravanan et al., Tribological properties of filler and green filler reinforced polymer composites. Mater. Today Proc. **50**, 2065–2072 (2022). https://doi.org/10.1016/j.matpr.2021.09.414

16. K.P. Toradmal, P.M. Waghmare, S.B. Sollapur, Three-point bending analysis of honeycomb sandwich panels: experimental approach. Int J Eng Tech 3(5):189–193 (2017)

17. S.B. Sollapur et al., Mechanical properties of bamboo fiber reinforced plastics. IJSART, vol 3. Issue 9 –SEPTEMBER 2017 ISSN [ONLINE]: 2395–1052, pp. 365–368

18. N. Shahrubudin, T.C. Lee, R.J.P.M. Ramlan, An overview on 3D printing technology: technological, materials, and applications. Procedia Manuf. **35**, 1286–1296 (2019)

19. U.A. Khilare, Investigation of residual stresses and its effect on mechanical behaviour of AISI310. J. Res. **02**(5), 42–46 (2016)

20. P.M. Waghmare, P.G. Bedmutha, Investigation of effect of hybridization and layering patterns on mechanical properties of banana and kenaf fibers reinforced epoxy biocomposite. Mater. Today Proc. **46**, 3220–3224 (2021)

21. R.C. Brooks, Origins, usage and production of screws: an historical perspective. Hist. Technol. Int. J. **8**(1), 51–76 (1991)

22. A. Blake, *Design of Mechanical Joints*, vol. 42 (CRC Press, 1985)

23. P.C. Sharath, P. Waghmare, Applications of additive manufacturing in biomedical and sports industry, in *Practical Implementations of Additive Manufacturing Technologies. Materials Horizons: From Nature to Nanomaterials*. ed. by S. Rajendrachari (Springer, Singapore, 2024). https://doi.org/10.1007/978-981-99-5949-5_13

24. G.R. Chate et al., Ceramic material coatings: emerging future applications, in *Advanced Ceramic Coatings for Emerging Applications*. (Elsevier, 2023), pp.3–17

25. A.J. Kinloch, C. Korenberg, K.T. Tan, J. Watts, *Durability of Structural Adhesive Joints* (Applied Science Publication, London, UK, 1983)

26. P. Yedamale, Brushless DC BLDC motor fundamentals. Microchip Technol. **20**(1), 3–15 (2003)

27. E. Kuantama, D. Craciun, I. Tarca, R. Tarca, *Quadcopter propeller design and performance analysis*. In New Advances in Mechanisms, Mechanical Transmissions and Robotics: Proceedings of The Joint International Conference of the XII International Conference on Mechanisms and Mechanical Transmissions (MTM) and the XXIII International Conference on Robotics (Robotics' 16), (Springer, 2017), pp. 269–277

28. A. Reichardt et al., Advances in additive manufacturing of metal-based functionally graded materials. Int. Mater. Rev. **66**(1), 1–29 (2021)

29. F.B. Teshome et al., Role of Pd interlayer on NiTi to Ti6Al4V laser welded joints: microstructural evolution and strengthening mechanisms. Mater. Des. **228**, 111845 (2023)

30. D.-M. Țura, S.-M. Zaharia, Design, additive manufacturing and testing of a quadcopter drone. Land Forces Acad Rev **28**(3), 245–254 (2023)

31. N.G. Siddeshkumar, R. Suresh, C.D. Prasad, L. Shivaram, N.H. Siddalingaswamy, Evolution of the surface quality and tool wear in the high speed turning of Al2219/n-B4C/MoS$_2$ metal matrix composites. Int. J. Cast Met. Res. (2023). https://doi.org/10.1080/13640461.2023.2285177

32. N. Praveen, U.S. Mallik, A.G. Shivasiddaramaiah, N. Nagabhushana, C.D. Prasad, S. Kollur, Effect of CNC end milling parameters on Cu–Al–Mn ternary shape memory alloys using Taguchi method. J. Inst. Eng. (India) Ser. D (2023). https://doi.org/10.1007/s40033-023-00579-3

33. C.D. Prasad, S. Kollur, C.R. Aprameya, T.V. Chandramouli, T. Jagadeesha, B.N. Prashanth, Investigations on tribological and microstructure characteristics of WC-12Co/FeNiCrMo composite coating by HVOF process. JOM J. Miner. Met. Mater. Soc. (TMS) (2023). https://doi.org/10.1007/s11837-023-06242-2

34. S. Gotagunaki, V.S. Mudakappanavar, R. Suresh, C.D. Prasad, Studies on the mechanical properties and wear behavior of an AZ91D magnesium metal matrix composite utilizing the stir casting method. Metallogr. Microstruct. Anal. (2023). https://doi.org/10.1007/s13632-023-01017-2

35. C. Manjunatha, T.N. Sreenivasa, P. Sanjay, C.D. Prasad, Optimization of friction stir welding parameters to enhance weld nugget hardness in AA6061-B$_4$C composite material. J. Inst. Eng. (India) Ser. D (2023). https://doi.org/10.1007/s40033-023-00562-y

36. C.D. Prasad, S. Kollur, M. Nusrathulla, G. Satheesh Babu, M.B. Hanamantraygouda, B.N. Prashanth, N. Nagabhushana, Characterisation and wear behaviour of SiC reinforced FeNiCrMo composite coating by HVOF process. Trans. IMF (2023). https://doi.org/10.1080/00202967.2023.2246259

37. G.S. Kulkarni, N.G. Siddeshkumar, C.D. Prasad, L. Shankar, R. Suresh, Drilling of GFRP with liquid silicon rubber reinforced with fine aluminium powder on hole surface quality and tool wear using DOE. J. Bio Tribo-Corros. **9**, 53 (2023). https://doi.org/10.1007/s40735-023-00771-8

38. N. Praveen, U.S. Mallik, A.G. Shivasiddaramaih, R. Suresh, C.D. Prasad, L. Shivaramu, Synthesis and wire EDM characteristics of Cu–Al–Mn ternary shape memory alloys using Taguchi method. J. Inst. Eng. (India) Ser. D (2023). https://doi.org/10.1007/s40033-023-00501-x

39. G.M.S. Reddy, C.D. Prasad, S. Kollur, A. Lakshmikanthan, R. Suresh, C.R. Aprameya, Investigation of high temperature erosion behaviour of NiCrAlY/TiO$_2$ plasma coatings on titanium substrate. JOM J. Miner. Met. Mater. Soc. (TMS) (2023). https://doi.org/10.1007/s11837-023-05894-4

40. N. Praveen, U.S. Mallik, A.G. Shivasiddaramaih, R. Suresh, L. Shivaramu, C.D. Prasad, M. Gupta, Design and analysis of shape memory alloys using optimization techniques. Adv. Mater. Process. Technol. (2023). https://doi.org/10.1080/2374068X.2023.2208021

41. G.M.S. Reddy, C.D. Prasad, P. Patil, N. Kakur, M.R. Ramesh, High temperature erosion performance of NiCrAlY/Cr$_2$O$_3$/YSZ plasma spray coatings. Trans. IMF (2023). https://doi.org/10.1080/00202967.2023.2208899

42. H. Sharanabasva, C.D. Prasad, M.R. Ramesh, Characterization and wear behavior of NiCrMoSi microwave cladding. J. Mater. Eng. Perform. (2023). https://doi.org/10.1007/s11665-023-07998-z

43. G. Madhusudana Reddy, C.D. Prasad, P. Patil, N. Kakur, M.R. Ramesh, Investigation of plasma sprayed NiCrAlY/Cr$_2$O$_3$/YSZ coatings on erosion performance of MDN 420 steel substrate at elevated temperatures. Int. J. Surf. Sci. Eng. **17**(3), 180–194 (2023). https://doi.org/10.1504/IJSURFSE.2023.10054266

44. H. Sharanabasva, C.D. Prasad, M.R. Ramesh, Effect of Mo and SiC reinforced NiCr microwave cladding on microstructure,

mechanical and wear properties. J. Inst. Eng. (India) Ser. D (2023). https://doi.org/10.1007/s40033-022-00445-8

45. G.M.S. Reddy, C.D. Prasad, G. Shetty, M.R. Ramesh, T. Nageswara Rao, P. Patil, Investigation of thermally sprayed NiCrAlY/TiO$_2$ and NiCrAlY/Cr$_2$O$_3$/YSZ cermet composite coatings on titanium alloys. Eng. Res. Express **4**, 025049 (2022). https://doi.org/10.1088/2631-8695/ac7946

46. G.M.S. Reddy, C.D. Prasad, P. Patil, N. Kakur, M.R. Ramesh, Elevated temperature erosion performance of plasma sprayed NiCrAlY/TiO$_2$ coating on MDN 420 steel substrate. Surf. Topogr. Metrol. Prop.Topogr. Metrol. Prop. **10**, 025010 (2022). https://doi.org/10.1088/2051-672X/ac6a6e

47. G. Madhusudana Reddy, C.D. Prasad, G. Shetty, M.R. Ramesh, T. Nageswara Rao, P. Patil, High temperature oxidation behavior of plasma sprayed NiCrAlY/TiO$_2$ & NiCrAlY /Cr$_2$O$_3$/YSZ coatings on titanium alloy. Weld. World (2022). https://doi.org/10.1007/s40194-022-01268-7

48. C.D. Prasad, S. Lingappa, S. Joladarashi, M.R. Ramesh, B. Sachin, Characterization and sliding wear behavior of CoMoCrSi+Flyash composite cladding processed by microwave irradiation. Mater. Today Proc. **46**, 2387–2391 (2021). https://doi.org/10.1016/j.matpr.2021.01.156

49. T. Naik, M. Mathapathi, C.D. Prasad, H.S. Nithin, M.R. Ramesh, Effect of laser post treatment on microstructural and sliding wear behavior of HVOF sprayed NiCrC and NiCrSi coatings. Surf. Rev. Lett.Lett. **29**(1), 225000 (2022). https://doi.org/10.1142/S0218625X2250007X

50. G.M.S. Reddy, C.D. Prasad, G. Shetty, M.R. Ramesh, T. Nageswara Rao, P. Patil, High temperature oxidation studies of plasma sprayed NiCrAlY/TiO$_2$ & NiCrAlY /Cr$_2$O$_3$/YSZ cermet composite coatings on MDN-420 special steel alloy. Metall. Microstruct. Anal. **10**, 642–651 (2021). https://doi.org/10.1007/s13632-021-00784-0

51. C.D. Prasad, S. Joladarashi, M.R. Ramesh, M.S. Srinath, B.H. Channabasappa, Microstructure and tribological behavior of flame sprayed and microwave fused CoMoCrSi/CoMoCrSi-Cr$_3$C$_2$ coatings. Mater. Res. Express **6**, 026512 (2019). https://doi.org/10.1088/2053-1591/aaebd9

52. M. Mathapati, K. Amate, C.D. Prasad, M.L. Jayavardhana, T. Hemanth Raju, A review on fly ash utilization. Mater. Today Proc. **50**(5), 1535–1540 (2022). https://doi.org/10.1016/j.matpr.2021.09.106

53. R. Dinesh, R. Raykar, T.L. Rakesh, M.G. Prajwal, S.M. Lingappa, C.D. Prasad, Feasibility study on MoCoCrSi/ WC-Co cladding developed on austenitic stainless steel using microwave hybrid heating. J. Min. Met. Fuels (2021). https://doi.org/10.18311/jmmf/2021/30113

54. C.D. Prasad, S. Joladarashi, M.R. Ramesh, M.S. Srinath, B.H. Channabasappa, Effect of microwave heating on microstructure and elevated temperature adhesive wear behavior of HVOF deposited CoMoCrSi–Cr$_3$C$_2$ composite coating. Surf. Coat. Technol. **374**, 291–304 (2019). https://doi.org/10.1016/j.surfcoat.2019.05.056

55. G. Madhu, K.M. Mrityunjaya Swamy, D.A. Kumar, C.D. Prasad, U. Harish, Evaluation of hot corrosion behavior of HVOF thermally sprayed Cr$_3$C$_2$–35NiCr coating on SS 304 boiler tube steel. Am. Inst. Phys. **2316**, 030014 (2021). https://doi.org/10.1063/5.0038279

56. M.S. Reddy, C.D. Prasad, P. Patil, M.R. Ramesh, N. Rao, Hot corrosion behavior of plasma sprayed NiCrAlY/TiO$_2$ and NiCrAlY/Cr$_2$O$_3$/YSZ cermets coatings on alloy steel. Surf.

57. C.D. Prasad, S. Joladarashi, M.R. Ramesh, M.S. Srinath, Microstructure and tribological resistance of flame sprayed CoMoCrSi/WC-CrC-Ni and CoMoCrSi/WC-12Co composite coatings remelted by microwave hybrid heating. J. Bio Tribo-Corros. **6**, 124 (2020). https://doi.org/10.1007/s40735-020-00421-3

58. C.D. Prasad, S. Joladarashi, M.R. Ramesh, Comparative investigation of HVOF and flame sprayed CoMoCrSi coating. Am. Inst. Phys. **2247**, 050004 (2020). https://doi.org/10.1063/5.0003883

59. C.D. Prasad, A. Jerri, M.R. Ramesh, Characterization and sliding wear behavior of iron based metallic coating deposited by HVOF process on low carbon steel substrate. J. Bio Tribo-Corros. **6**, 69 (2020). https://doi.org/10.1007/s40735-020-00366-7

60. H.S. Nithin, K.M. Nishchitha, D.G. Pradeep, C.D. Prasad, M. Mathapati, Comparative analysis of CoCrAlY coatings at high temperature oxidation behavior using different reinforcement composition profiles. Weld. World **67**, 585–592 (2023). https://doi.org/10.1007/s40194-022-01405-2

61. C.D. Prasad, S. Joladarashi, M.R. Ramesh, M.S. Srinath, B.H. Channabasappa, Comparison of high temperature wear behavior of microwave assisted HVOF sprayed CoMoCrSi–WC–CrC–Ni/WC–12Co composite coatings. SILICON **12**, 3027–3045 (2020). https://doi.org/10.1007/s12633-020-00398-1

62. K.G. Girisha, R. Rakesh, C.D. Prasad, K.V. Sreenivas Rao, Development of corrosion resistance coating for AISI 410 grade steel. Appl. Mech. Mater. **813–814**, 135–139 (2015). https://doi.org/10.4028/www.scientific.net/AMM.813-814.135

63. C.D. Prasad, S. Joladarashi, M.R. Ramesh, M.S. Srinath, B.H. Channabasappa, Development and sliding wear behavior of Co–Mo–Cr–Si cladding through microwave heating. SILICON **11**, 2975–2986 (2019). https://doi.org/10.1007/s12633-019-0084-5

64. C.D. Prasad, S. Joladarashi, M.R. Ramesh, M.S. Srinath, B.H. Channabasappa, Influence of microwave hybrid heating on the sliding Wear behaviour of HVOF sprayed CoMoCrSi coating. Mater. Res. Express **5**, 086519 (2018). https://doi.org/10.1088/2053-1591/aad44e

65. K.G. Girisha, C.D. Prasad, K.C. Anil, K.V. Sreenivas Rao, Dry sliding wear behaviour of Al2O3 coatings for AISI 410 grade stainless steel. Appl. Mech. Mater. **766–767**, 585–589 (2015). https://doi.org/10.4028/www.scientific.net/AMM.766-767.585

66. C.D. Prasad, S. Joladarashi, M.R. Ramesh, A. Sarkar, High temperature gradient cobalt based clad developed using microwave hybrid heating. Am. Inst. Phys. **1943**, 020111 (2018). https://doi.org/10.1063/1.5029687

67. K.G. Girisha, K.V. Sreenivas Rao, C.D. Prasad, Slurry erosion resistance of martenistic stainless steel with plasma sprayed Al$_2$O$_3$–40%TiO$_2$ coatings. Mater. Today Proc. **5**, 7388–7393 (2018). https://doi.org/10.1016/j.matpr.2017.11.409